Hyperscaling analysis of a disorder-induced ferromagnetic quantum critical point in $Ni_{1-x}Rh_x$ with $x = 0.375$

R.-Z. Lin and C.-L. Huang
Department of Physics and Center for Quantum Frontiers of Research & Technology (QFort), National Cheng Kung University, Tainan 701, Taiwan

(Received 29 November 2021; accepted 20 January 2022; published 31 January 2022)

Here, we report on a hyperscaling analysis of the thermodynamic measurements as a function of temperature and magnetic field for $Ni_{1-x}Rh_x$ with $x = 0.375$ where a ferromagnetic quantum critical point has been recently identified [Phys. Rev. Lett. **124**, 117203 (2020)]. The obtained critical exponents agree well with the theory proposed by Belitz, Kirkpatrick, and Vojta for a disorder tuned quantum critical point in the preasymptotic region.

DOI: 10.1103/PhysRevB.105.024429

I. INTRODUCTION

A magnetic quantum critical point (QCP) occurs when a second-order phase transition is suppressed to absolute zero by applying a nonthermal control parameter, such as pressure, magnetic field, strain, or chemical substitution [1]. A good deal of strange phenomena have been discovered in the vicinity of the QCP. These phenomena are often accompanied by a breakdown of Fermi-liquid (FL) theory, and in some cases, unconventional superconductivity [2,3]. It is still unclear whether the quantum fluctuation of the order parameter, the only relevant energy scale close to the QCP, intricately connects the quantum criticality and unconventional superconductivity [3–7]. Nevertheless, exploring new QCPs could potentially pave the way for deeper insight in understanding of the non-Fermi-liquid physics and shed light on the relation between the quantum fluctuations and unconventional superconductivity.

Successful tuning of a magnetic system towards the QCP has proven rarer in ferromagnets than in antiferromagnets, most probably due to the existence of multiple dynamical exponents in the former [8]. Although QCPs have been revealed in the ferromagnets $Zr_{1-x}Nb_xZn_2$, $SrCo_2(Ge_{1-x}P_x)_2$, $YbNi_4(P_{1-x}As_x)_2$, and $CeRh_6Ge_4$ [9–12], a decisive route to reach the ferromagnetic (FM) QCP remains ambiguous. A recent theory proposed by Belitz, Kirkpatrick, and Vojta (BKV) suggests one may restore the FM QCP by introducing an appropriate amount of quenched disorder [13–16]. To look for model systems to test the BKV theory, one shall start from one with a simple crystal structure to avoid structure complexity. In addition, an f-electron FM system is less appropriate compared to the d-electron ones, as the disorder also adjusts the competition between magnetic Ruderman-Kittel-Kasuya-Yosida (RKKY) interactions and the nonmagnetic Kondo effect in f-electron magnets [17,18]. Ni has a simple face-centered-cubic structure and is a three-dimensional d-electron ferromagnet with a Curie temperature $T_C \approx 627$ K [19,20]. The ordering temperature can be suppressed by alloying Ni with nonmagnetic or paramagnetic transition metals $Ni_{1-x}A_x$ [21–24]. Low-temperature quantum critical behavior has been extensively studied near the critical concentration x_c in $Ni_{1-x}Pd_x$ [25], $Ni_{1-x}V_x$ [26], and $Ni_{1-x}Rh_x$ [27]. The former two alloys did not exhibit QCPs, but showed randomness in magnetic interactions caused by disorder: Superparamagnetism was suggested to be responsible for the constant thermal expansion coefficient as $T \to 0$ in $Ni_{1-x}Pd_x$ [28], and additional disorder-induced fluctuations gave rise to a nonanalytic contribution to the free energy, forming the so-called Griffiths rare regions, in $Ni_{1-x}V_x$ [26]. Our previous work on $Ni_{1-x}Rh_x$ presented thermodynamic evidence for a disorder-induced FM QCP in the vicinity of $x_c = 0.375$ [see Fig. 1(a)] [27]. To the best of our knowledge, $Ni_{1-x}Rh_x$ is the only $Ni_{1-x}A_x$ alloy that exhibits a FM QCP. Moreover, it shows the first occurrence of a FM QCP with direct dilution of the d-electron magnetic site, leading $Ni_{1-x}Rh_x$ to hold a unique position among quantum critical materials.

Close to a QCP, universal relations among thermodynamic properties appear. That is, a set of critical exponents and the scaling functions are universal up to a certain symmetry and spatial dimensionality [29]. Here, we report a hyperscaling analysis of the low-temperature magnetization and specific heat data for $Ni_{1-x}Rh_x$ with $x = 0.375$, bearing all the features of a FM QCP [27]. The obtained scaling exponents are in line with the theoretical prediction for a FM fixed point in the asymptotic limit of high disorder [15,16]. This work reinforces the role of quenched disorder in tuning the FM transition continuously to absolute zero, as suggested by the BKV theory, providing a promising route to enlarge the portfolio of FM quantum critical materials, in addition to antiferromagnetic counterparts.

II. EXPERIMENTAL DETAILS

Polycrystalline $Ni_{1-x}Rh_x$ samples were prepared by arc melting high-purity Ni and Rh elements. The details of the sample characterization have been reported in our earlier

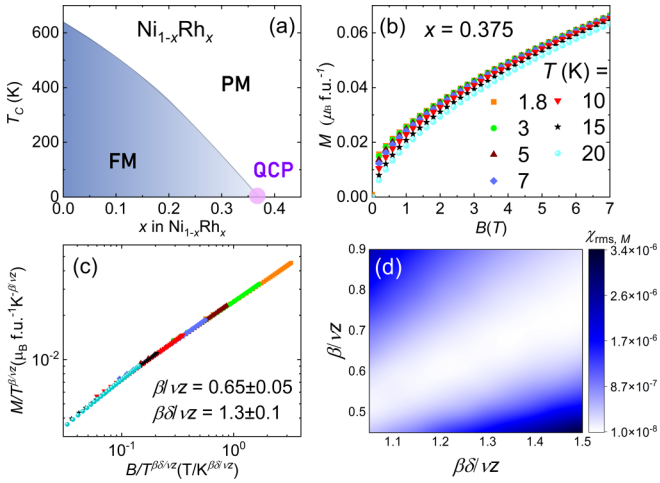

FIG. 1. (a) T_C-x phase diagram of $Ni_{1-x}Rh_x$. FM stands for a ferromagnetically ordered state and PM stands for a paramagnetically ordered state. The phase boundary between FM and PM is from Ref. [27] and references therein. (b) Isothermal magnetization M curves for the $x = 0.375$ sample. (c) Scaling of M as a function of T and B. (d) Mean square deviation $\chi_{\mathrm{rms},M}$ as a function of critical exponents $\beta/\nu z$ and $\beta\delta/\nu z$.

work [27]. Isothermal magnetization measurements were carried out between the temperatures $T = 1.8$ and 20 K and the magnetic fields $B = 0$ and 7 T using a Quantum Design (QD) magnetic property measurement system. Samples were field cooled at 7 T from high temperatures before performing the measurements. The specific heat was measured between $T = 0.05$ and 30 K and $B = 0$ and 14 T using a QD physical property measurement system equipped with a dilution refrigerator option.

III. RESULTS

The magnetic isotherms of $Ni_{1-x}Rh_x$ with $x = 0.375$ are shown in Fig. 1(b). $M(T, B)$ increases less rapidly with increasing T, suggesting the applicability of a scaling relation. At a QCP below the upper critical dimension, the scaling relation of the Gibbs free energy $\mathcal{F}(T, B)$ reads

$$\mathcal{F}(T, B) = b^{-(d+z)}\mathcal{F}(b^z T, b^{\beta\delta/\nu}B), \tag{1}$$

where b is an arbitrary scale factor, d is the spatial dimension, z is a dynamical exponent associated with the tuning parameter T, and $\beta\delta/\nu$ is the scaling exponent associated with the tuning parameter B [1]. Customarily, β describes the concentration dependence of the order parameter $m(r = x_c - x, T = B = 0) \propto r^\beta$, δ narrates the field dependence of $m(r = T = 0, B) \propto B^{1/\delta}$, and ν is the exponent obtained from the scaling relation of the diverging correlation length $\xi \propto |r|^{-\nu}$. For a FM system such as $Ni_{1-x}Rh_x$, the order parameter is the magnetization M. The field and temperature dependence of M in the vicinity of a QCP follows:

$$M(T, B) = -\frac{\partial \mathcal{F}}{\partial B} = b^{\beta\delta/\nu-(d+z)}M(b^z T, b^{\beta\delta/\nu}B). \tag{2}$$

If we choose $b^z T = T_0$ with a cutoff energy $k_B T_0$, one gets

$$\frac{M(T, B)}{T^{\beta/\nu z}} = \Phi\left(\frac{B}{T^{\beta\delta/\nu z}}\right), \tag{3}$$

indicating that $M/T^{\beta/\nu z}$ should be a universal function of $B/T^{\beta\delta/\nu z}$. Excellent scaling over three orders of magnitude of $B/T^{\beta\delta/\nu z}$ with $\beta/\nu z = 0.65 \pm 0.05$ and $\beta\delta/\nu z = 1.3 \pm 0.1$ is shown in Fig. 1(c). Due to domain effects, the data of low fields ($B < 1$ T) are omitted [30,31]. The trend of the scaling plot is similar to those in $UCo_{1-x}Fe_xGe$ and UTe_2 [3,31]. In the present study the function of Φ is unknown, and we therefore fit the data using a polynomial to determine the goodness of scaling. For values of $\beta/\nu z$ between 0.45 and 0.9 and $\beta\delta/\nu z$ between 1.05 and 1.5 with a step size of 0.05, the determination of exponents is through the smallest root mean square deviation $\chi_{\mathrm{rms},M}$. The minimal $\chi_{\mathrm{rms},M}$ occurs along the diagonal where the ratio of $\beta/\nu z$ and $\beta\delta/\nu z$, i.e., δ, is $\sim$2, as shown in Fig. 1(d). This result alone, however, could not decide other critical exponents. We hence resort to a hyperscaling analysis of the specific heat that allows a decisive determination of d/z and $\beta\delta/\nu z$.

Figure 2(a) shows the temperature dependence of the total specific heat coefficient C/T in different fields. Upon cooling, zero field C/T first decreases down to $\sim$10 K and then increases slightly toward low T, manifesting quantum fluctuations close to a FM QCP. As the field increases, the tendency towards FL behavior $C/T = \mathrm{const}$ as $T \to 0$ is gradually restored. Such a recovery of FL behavior has been observed in many antiferromagnetic and FM QCPs as the system is tuned away from the QCP and toward a magnetically disordered phase [1,8].

The total specific heat C can be expressed by $C = C_e + C_{\mathrm{ph}}$, where C_e and C_{ph} are electronic and phonon contributions to the specific heat, respectively. At relatively high T where no magnetic order is involved, $C_e = \gamma_0 T$ where γ_0 is the Sommerfeld coefficient. For $x < x_c$ in $Ni_{1-x}Rh_x$, the split of the itinerant conduction d electron bands causes FM order based on Stoner's model [32]. When $x \to x_c$, quantum fluctuations emerge and destroy the magnetic order. Both FM order and quantum fluctuations (sometimes intertwined) renormalize C_e at low T and must be treated with caution. First of all, we need to properly extract C_{ph} by focusing on a relatively high T region where the above-mentioned contributions to C_e are negligible, and fit the C/T data between $T = 15$ and 30 K with a sum of a constant γ_0 and an integral Debye term for C_{ph}. The obtained C_{ph} is shown as a solid line in Fig. 2(a). After subtracting C_{ph} from C, the temperature dependence of C_e/T with increasing B is shown in Fig. 2(b). The data scatter below 0.4 K due to the fact that C_e/T only amounts to $\sim$15–20 mJ/mol K^2, comparable with the value of exchange-enhanced systems without quantum fluctuations [33], and the gradual decrease of C_e/T from $B = 0$ to 14 T is less than 20%, close to the resolution limit of the calorimeter. The hyperscaling relation of the quantum critical part of the specific heat is given by

$$C_{\mathrm{cr}}(T, B) = -T\frac{\partial^2 \mathcal{F}}{\partial T^2} = b^{-d}C_{\mathrm{cr}}(b^z T, b^{\beta\delta/\nu}B). \tag{4}$$

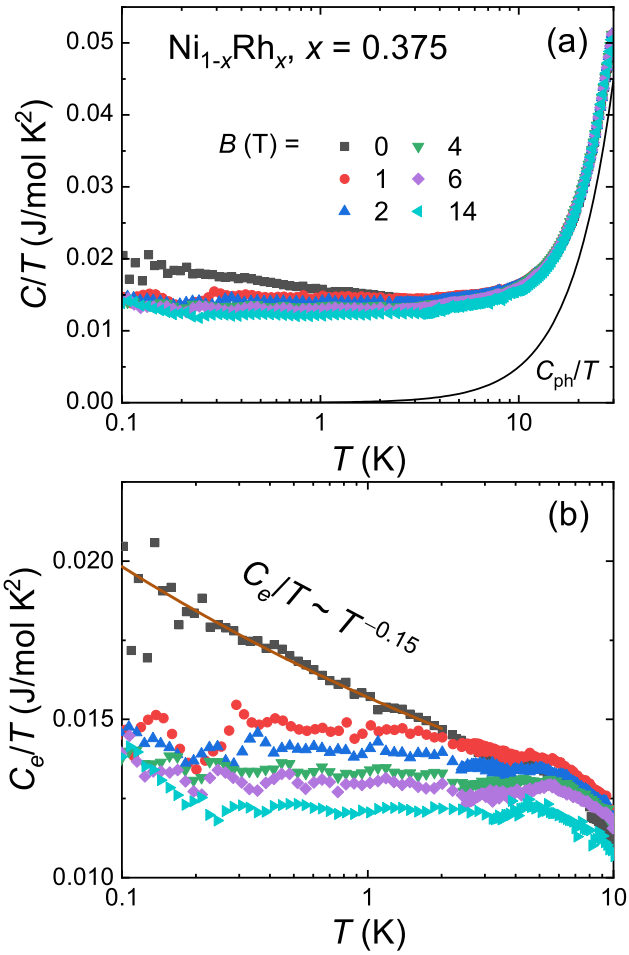

FIG. 2. (a) Temperature dependence of specific heat in different magnetic fields of $Ni_{1-x}Rh_x$ with $x = 0.375$, plotted as C/T vs T in semilogarithmic scale. The solid line represents the phonon contribution to the specific heat C_{ph}/T. (b) The electronic contribution to the specific heat C_e/T. The solid line represents a fit of $\gamma_0 + aT^{d/z-1}$ between 0.1 and 2 K. See text for details.

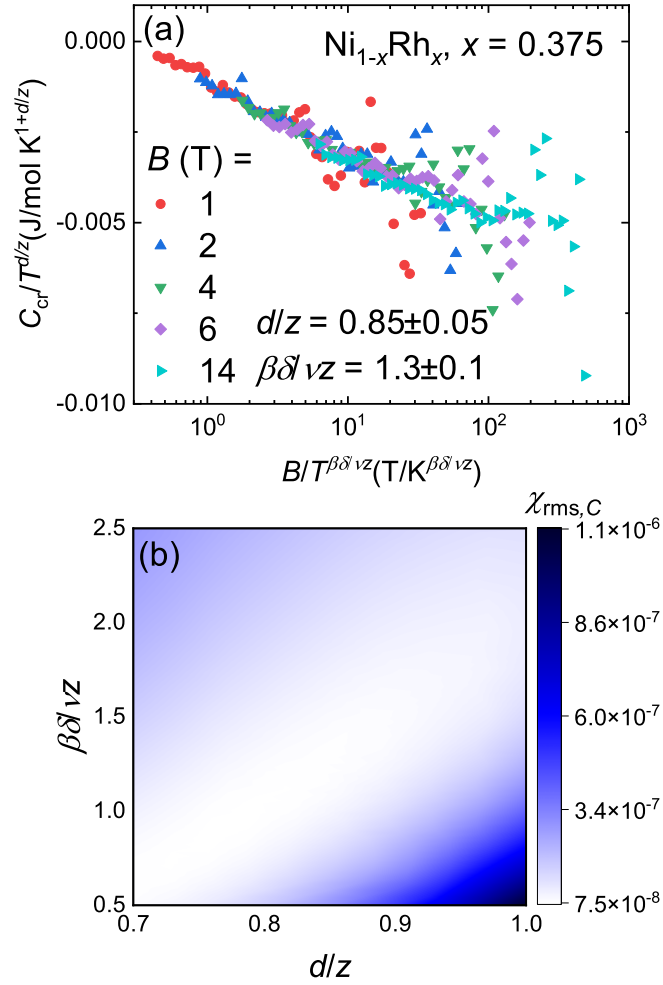

FIG. 3. (a) Scaling of C_{cr} as a function of T and B of $Ni_{1-x}Rh_x$ with $x = 0.375$. (b) $\chi_{rms,C}$ as a function of critical exponents d/z and $\beta\delta/\nu z$.

We choose $b^z T = T_0$ again and Eq. (4) becomes

$$\frac{C_{cr}(T,B)}{T^{d/z}} = \Psi\left(\frac{B}{T^{\beta\delta/\nu z}}\right). \tag{5}$$

In order to check the T and B scaling of the specific heat, we plot $[C(T,B) - C(T,0)]/T^{d/z}$ vs $B/T^{\beta\delta/\nu z}$ in Fig. 3(a) to eliminate the noncritical quasiparticle contribution to C_e [30]. We vary $d/z = 0.65$–1 with a step size of 0.05 and $\beta\delta/\nu z = 0.5$–2.5 with a step size of 0.1, and use a polynomial fit to determine the combination of critical exponents which allow the data to collapse onto a universal curve. A local minimum in $\chi_{rms,C}(d/z, \beta\delta/\nu z)$ confining $\beta\delta/\nu z$ to be 1.0–1.5 with $d/z = 0.75$–0.9 is found [Fig. 3(b)].

Finally, Eq. (5) hints that the zero-field specific heat $C_{cr}(T,0) = T^{d/z}\Psi(0)$, which allows an unequivocal determination of d/z. Figure 2(b) demonstrates the data between 2 and 0.1 K can be well described by $C_e/T = \gamma_0 + aT^{d/z-1}$ with $\gamma_0 = 5.7$ mJ/mol K^2, $a = 10$ mJ/mol K$^{1.85}$, and $d/z = 0.85$. With this last piece of evidence, we are able to scale $C_{cr}(T,B)$. Apart from the low T scattered data due to small C_{cr}, scaling works over three orders of magnitude in $B/T^{\beta\delta/\nu z}$ with $\beta\delta/\nu z = 1.3 \pm 0.1$ [Fig. 3(a)].

IV. DISCUSSIONS

In our previous work, a logarithmic divergence was applied to describe the zero-field C/T [27], which seems inconsistent with the power law found in Fig. 2(b). This reflects a fact that a logarithmic divergence could be hardly distinguished from a negative power law with a very small exponent $d/z - 1$, as the former is just a $d/z - 1 = 0$ limit of the latter. By analyzing the zero-field C/T data alone, one may not be able to differentiate one from the other. In this paper, we can unambiguously conclude the power law better describes zero-field $C(T)$, through a consistent hyperscaling analysis on temperature and field dependence of magnetization and specific heat.

From a magnetization scaling analysis we have derived $\delta = 2.0 \pm 0.2$. This value is small compared with the mean-field Hertz-Millis-Moriya theory either for clean or disordered systems ($\delta = 3$) which is usually enhanced via critical fluctuations [30,34–36]. The dynamical critical exponent $z = 3.5 \pm 0.2$ can be deduced from $d/z = 0.85 \pm 0.05$ if we assume

TABLE I. Comparison between experiments and theory.

	Current result	Hertz's fixed point in the dirty limit	BKV's theory	BKV's theory in the preasymptotic region
δ	2.0 ± 0.2	3	1.5	1.8
z	3.5 ± 0.2	4	3	3.7

$d = 3$. Such an assumption is deemed to be reasonable as the crystal structure of $Ni_{1-x}Rh_x$ is face centered cubic.

Our experimental results are summarized and compared with theoretical predictions in Table I. The obtained δ and z values are not comparable with the Hertz's model even in the dirty limit [1]. It is well known that Hertz's fixed point is unstable against the existence of dangerous irrelevant variables [8]. Upon utilizing an appropriate amount of chemical disorder, BKV suggested one could restore the FM QCP and the critical exponents $\delta = \frac{d}{2} = 1.5$ and $z = d = 3$ [15,16]. When a system is asymptotically close to the FM QCP, both critical exponents are modified by an effective exponent λ that depends on the distance from a QCP. BKV predicted that in $d = 3$, $\lambda = 2/3$ in a large region, and hence $\delta_{\text{asym}} = \frac{d+\lambda}{2} = 1.8$ and $z_{\text{asym}} = d + \lambda = 3.7$. Our results agree well with the BKV theory in the preasymptotic region, which implies that $x = 0.375$ locates very close to the FM QCP of $Ni_{1-x}Rh_x$ in which quantum fluctuations lead to divergence (see our previous work [27]) and hyperscaling behavior of thermodynamic properties.

The key concept in the BKV theory to reach a FM QCP is via an appropriate amount of chemical disorder. If the disorder effect is too strong, the QCP is avoided and spin glassiness may appear near the boundary of the quantum phase transition between the FM and PM states [15,16,37]. Experimentally, however, it is difficult to gauge the degree of disorder from different sources. For example, how do we judge that the amount of disorder in $Ni_{1-x}Pd_x$ and $Ni_{1-x}V_x$ is larger than that in $Ni_{1-x}Rh_x$? Conventional crystal structure analysis tools, such as x-ray diffraction, an electron probe microanalyzer, and scanning electron microscopy, cannot give a clue to this question. One may turn to utilize the probe of magnetic properties with elemental selectivity, e.g., x-ray magnetic circular dichroism (XMCD), to study the magnetic homogeneity. Usually, when a FM element is alloyed with a nonmagnetic metal A, its PM effective moment μ_{eff} derived from a Curie-Weiss fit at high T decreases as the concentration of A increases. $Ni_{1-x}Rh_x$ is unique among $Ni_{1-x}A_x$ alloys as it is the only system in which μ_{eff} remains almost constant as $x \to x_c$ [23]. This reflects a fact that magnetism in $4d$ Rh atoms is largely enhanced when Rh is surrounded by Ni atoms [38]. XMCD measurements on $Ni_{1-x}A_x$ alloys close to x_c may reveal the magnetic behavior in the local environment either on the Ni or A site, and show the difference of the homogeneity of magnetic properties among different systems. This testing method, if it works, will further justify the applicability of the BKV theory and serve as a useful guidance when exploring new FM QCPs.

ACKNOWLEDGMENTS

We thank Dr. M.-K. Lee and C.-C. Yang at PPMS-16T and SQUID VSM Labs, Instrumentation Center, National Cheng Kung University (NCKU) for technical support. We thank D. Belitz and T. R. Kirkpatrick for useful discussions. C.L.H. would like to thank E. Morosan for her kind support in the earlier stage of this study. This work is supported by the Ministry of Science and Technology in Taiwan (Grants No. MOST 109-2112-M-006-026-MY3 and No. MOST 110-2124-M-006-009) and the Higher Education Sprout Project, Ministry of Education to the Headquarters of University Advancement at NCKU.

[1] H. v. Löhneysen, A. Rosch, M. Vojta, and P. Wölfle, Rev. Mod. Phys. **79**, 1015 (2007).
[2] E. Schuberth, M. Tippmann, L. Steinke, S. Lausberg, A. Steppke, M. Brando, C. Krellner, C. Geibel, R. Yu, Q. Si *et al.*, Science **351**, 485 (2016).
[3] S. Ran, C. Eckberg, Q.-P. Ding, Y. Furukawa, T. Metz, S. R. Saha, I.-L. Liu, M. Zic, H. Kim, J. Paglione *et al.*, Science **365**, 684 (2019).
[4] N. D. Mathur, F. M. Grosche, S. R. Julian, I. R. Walker, D. M. Freye, R. K. W. Haselwimmer, and G. G. Lonzarich, Nature (London) **394**, 39 (1998).
[5] P. Monthoux, D. Pines, and G. G. Lonzarich, Nature (London) **450**, 1177 (2007).
[6] Y. Nakai, T. Iye, S. Kitagawa, K. Ishida, H. Ikeda, S. Kasahara, H. Shishido, T. Shibauchi, Y. Matsuda, and T. Terashima, Phys. Rev. Lett. **105**, 107003 (2010).
[7] B. Keimer, S. A. Kivelson, M. R. Norman, S. Uchida, and J. Zaanen, Nature (London) **518**, 179 (2015).
[8] M. Brando, D. Belitz, F. M. Grosche, and T. R. Kirkpatrick, Rev. Mod. Phys. **88**, 025006 (2016).
[9] D. A. Sokolov, M. C. Aronson, W. Gannon, and Z. Fisk, Phys. Rev. Lett. **96**, 116404 (2006).
[10] S. Jia, P. Jiramongkolchai, M. R. Suchomel, B. H. Toby, J. G. Checkelsky, N. P. Ong, and R. J. Cava, Nat. Phys. **7**, 207 (2011).
[11] A. Steppke, R. Küchler, S. Lausberg, E. Lengyel, L. Steinke, R. Borth, T. Lühmann, C. Krellner, M. Nicklas, C. Geibel *et al.*, Science **339**, 933 (2013).
[12] B. Shen, Y. Zhang, Y. Komijani, M. Nicklas, R. Borth, A. Wang, Y. Chen, Z. Nie, R. Li, X. Lu *et al.*, Nature (London) **579**, 51 (2020).
[13] D. Belitz, T. R. Kirkpatrick, and T. Vojta, Phys. Rev. Lett. **82**, 4707 (1999).
[14] Y. Sang, D. Belitz, and T. R. Kirkpatrick, Phys. Rev. Lett. **113**, 207201 (2014).
[15] T. R. Kirkpatrick and D. Belitz, Phys. Rev. Lett. **113**, 127203 (2014).
[16] T. R. Kirkpatrick and D. Belitz, Phys. Rev. B **91**, 214407 (2015).
[17] G. R. Stewart, Rev. Mod. Phys. **73**, 797 (2001).
[18] G. R. Stewart, Rev. Mod. Phys. **78**, 743 (2006).
[19] D. G. Howard, B. D. Dunlap, and J. G. Dash, Phys. Rev. Lett. **15**, 628 (1965).

[20] Y. Kraftmakher, Eur. J. Phys. **18**, 448 (1997).
[21] K. P. Gupta, C. H. Cheng, and P. A. Beck, Phys. Rev. **133**, A203 (1964).
[22] W. F. Brinkman, E. Bucher, H. J. Williams, and J. P. Maita, J. Appl. Phys. **39**, 547 (1968).
[23] F. Bölling, Phys. Kondens. Mater. **7**, 162 (1968).
[24] I. P. Gregory and D. E. Moody, J. Phys. F: Met. Phys. **5**, 36 (1975).
[25] M. Nicklas, M. Brando, G. Knebel, F. Mayr, W. Trinkl, and A. Loidl, Phys. Rev. Lett. **82**, 4268 (1999).
[26] S. Ubaid-Kassis, T. Vojta, and A. Schroeder, Phys. Rev. Lett. **104**, 066402 (2010).
[27] C.-L. Huang, A. M. Hallas, K. Grube, S. Kuntz, B. Spieß, K. Bayliff, T. Besara, T. Siegrist, Y. Cai, J. Beare, G. M. Luke, E. Morosan, Phys. Rev. Lett. **124**, 117203 (2020).
[28] R. Küchler, P. Gegenwart, F. Weickert, N. Oeschler, T. Cichorek, M. Nicklas, N. Carocca-Canales, C. Geibel, and F. Steglich, Phys. B: Condens. Matter **378-380**, 36 (2006).
[29] P. C. Hohenberg and B. I. Halperin, Rev. Mod. Phys. **49**, 435 (1977).
[30] C.-L. Huang, D. Fuchs, M. Wissinger, R. Schneider, M. C. Ling, M. S. Scheurer, J. Schmalian, and H. v. Löhneysen, Nat. Commun. **6**, 8188 (2015).
[31] K. Huang, S. Eley, P. F. S. Rosa, L. Civale, E. D. Bauer, R. E. Baumbach, M. B. Maple, and M. Janoschek, Phys. Rev. Lett. **117**, 237202 (2016).
[32] J. M. Santiago, C.-L. Huang, and E. Morosan, J. Phys.: Condens. Matter **29**, 373002 (2017).
[33] A. Tari, *The Specific Heat of Matter at Low Temperatures* (Imperial College Press, London, 2003).
[34] J. A. Hertz, Phys. Rev. B **14**, 1165 (1976).
[35] A. J. Millis, Phys. Rev. B **48**, 7183 (1993).
[36] T. Moriya, *Spin Fluctuations in Itinerant Electron Magnetism* (Springer, Berlin, 1985).
[37] T. Vojta, J. Low Temp. Phys. **161**, 299 (2010).
[38] V. V. Krishnamurthy, S. N. Mishra, M. R. Press, P. L. Paulose, S. H. Devare, and H. G. Devare, Phys. Rev. B **49**, 6726 (1994).